Published in final edited form as:
J Neurochem. 2007 December ; 103(6): 2212–2223. doi:10.1111/j.1471-4159.2007.04906.x.

Superoxide dismutase/catalase mimetics but not MAP kinase inhibitors are neuroprotective against oxygen/glucose deprivation-induced neuronal death in hippocampus

Miou Zhou, **Reymundo Dominguez**, and **Michel Baudry**
Neuroscience Program, University of Southern California, Los Angeles, California, USA

Abstract

Although oxygen/glucose deprivation (OGD) has been widely used as a model of ischemic brain damage, the mechanisms underlying acute neuronal death in this model are not yet well understood. We used OGD in acute hippocampal slices to investigate the roles of reactive oxygen species and of the mitogen-activated protein kinases (MAPKs) in neuronal death. In particular, we tested the neuroprotective effects of two synthetic superoxide dismutase/catalase mimetics, EUK-189 and EUK-207. Acute hippocampal slices prepared from 2-month-old or postnatal day 10 rats were exposed to oxygen and glucose deprivation for 2 h followed by 2.5 h reoxygenation. Lactate dehydrogenase (LDH) release in the medium and propidium iodide (PI) uptake were used to evaluate cell viability. EUK-189 or EUK-207 applied during the OGD and reoxygenation periods decreased LDH release and PI uptake in slices from 2-month-old rats. EUK-189 or EUK-207 also partly blocked OGD-induced ATP depletion and extracellular signal-regulated kinases 1 and 2 (ERK1/2) dephosphorylation, and completely eliminated reactive oxygen species generation. The MEK inhibitor U0126 applied together with EUK-189 or EUK-207 completely blocked ERK1/2 activation, but had no effect on their protective effects against OGD-induced LDH release. U0126 alone had no effect on OGD-induced LDH release. EUK-207 had no effect on OGD-induced p38 or c-Jun N-terminal kinase dephosphorylation, and when the p38 inhibitor SB203580 was applied together with EUK-207, it had no effect on the protective effects of EUK-207. SB203580 alone had no effect on OGD-induced LDH release either. In slices from p10 rats, OGD also induced high-LDH release that was partly reversed by EUK-207; however, neither OGD nor EUK-207 produced significant changes in ERK1/2 and p38 phosphorylation. OGD-induced spectrin degradation was not modified by EUK-189 or EUK-207 in slices from p10 or 2-month-old rats, suggesting that their protective effects was not mediated through inhibition of calpain activation. Thus, both EUK-189 and EUK-207 provide neuroprotection in acute ischemic conditions, and this effect is related to elimination of free radical formation and partial reversal of ATP depletion, but not mediated by the activation or inhibition of the MEK/ERK or p38 pathways, or inhibition of calpain activation.

Keywords

calpain; hippocampus; ischemia; MAP kinase; neurodegeneration; oxygen/glucose deprivation; reactive oxygen species

Cerebral ischemia is the disruption of blood supply to the brain and is the third leading cause of death in the United States (Gupta and Sharma 2006). Ischemia triggers a variety of

Address correspondence and reprint requests to Michel Baudry, HNB534, USC, Los Angeles, CA 90089-2520, USA. Baudry@usc.edu.

pathological events, including excitotoxicity, inflammation, delayed neuronal dysfunction and cell death, and has also been implicated in Alzheimer's and other neurodegenerative diseases (reviewed in Koistinaho and Koistinaho 2005; Zipp and Aktas 2006). The mechanisms underlying ischemic neuronal death are not completely understood. Cerebral ischemia induces over-activation of glutamate receptors, production of oxygen free radicals, pathological increase in intracellular calcium concentration, rapid ATP depletion, and activation of various proteolytic enzymes (Karadottir *et al.* 2005; Al Majed *et al.* 2006; Kovacs *et al.* 2006). Drugs that provide neuroprotection against ischemia-induced cell death might act on any of those downstream events following ischemia.

Oxygen/glucose deprivation (OGD) in *in vitro* preparations is widely used as a model of ischemic conditions, as it triggers all the above-mentioned processes and results in neuronal damage. The present experiments were designed to test the involvement of some of these mechanisms in OGD-induced cell death in acute hippocampal slices. Participation of reactive oxygen species was tested by using two salen-manganese complexes, EUK-189 and EUK-207, which have been shown to act as synthetic superoxide dismutase/catalase mimetics, and thus eliminate both superoxide and hydrogen peroxide (Doctrow *et al.* 2003). The compounds have shown efficacy in different disease models associated with reactive oxygen species (ROS) formation. For example, they protected hippocampal slices from hypoxia-, acidosis-, and β-amyloid protein- (Aβ) induced cell death, reduced brain infarction volume in a rat focal cerebral ischemia model, blocked neurotoxicity produced by kainic acid or MPP+, prolonged lifespan of *Caenorhabditis elegans* and sod2 null mouse, and reversed cognitive deficits and protein oxidation in 11-month old mice (Musleh *et al.* 1994; Baker *et al.* 1998; Rong *et al.* 1999; Melov *et al.* 2000, 2001; Pong *et al.* 2001; Doctrow *et al.* 2002; Liu *et al.* 2003; Peng *et al.* 2005). Different compounds differ in their SOD activity, catalase activity, lipophilicity and stability, and all these properties determine their neuroprotective efficiency.

Another type of intracellular pathways frequently implicated in mechanisms of cell death/cell survival consists of the family of mitogen-activated protein kinases (MAPKs), which comprises the extracellular signal-regulated kinases 1 and 2 (ERK1/2), p38, and stress-activated protein kinases (SAP-Ks)/c-Jun N-terminal kinase (JNK). In particular, the role of ERK1/2 in ischemia remains ambiguous, as ERK1/2 has been shown to be either activated or inactivated following ischemia and reperfusion depending on the models, and activation of this pathway has been reported to promote neuronal survival as well as cell death (Murray *et al.* 1998; Namura *et al.* 2001; Fahlman *et al.* 2002; Zhu *et al.* 2005). MEK1/2 is a serine/threonine protein kinase that activates ERK1/2, and MEK1/2 inhibitors, such as U0126 and SL327 are widely used to study the role of MEK/ERK in different animal ischemia models (Namura *et al.* 2001; Wang *et al.* 2003). P38 and JNK are also involved in cellular responses to stress, such as cerebral ischemia, and p38 inhibition has been shown to provide neuronal protection in cerebral ischemia (Sugino *et al.* 2000b; Barone *et al.* 2001), although p38 activation is also involved in neuronal protection against some insults (Lin *et al.* 2006; Claytor *et al.* 2007).

Calpains are calcium-activated proteases implicated in physiological conditions, such as synaptic modifications during neuronal development and adult synaptic plasticity, and also in pathological states including excitotoxic neuronal death, oxidative stress and free radical generation, Alzheimer disease and several neurodegenerative conditions (Lynch and Baudry 1987; Ray *et al.* 2000; Kelly and Ferreira 2006). Calpain is also activated in brain ischemia and reperfusion (Yamashima *et al.* 2003), and the calpain inhibitor MDL 28170 has been reported to protect newborn rat brain from hypoxic ischemia by decreasing both necrosis and apoptosis (Kawamura *et al.* 2005). Our results indicate that reactive oxygen species play

a critical role in acute neuronal death resulting from ischemia, while neither the MAPK pathways or calpain activation contributes to neuronal death, at least in adult rats.

Materials and methods

Materials

EUK-189 and EUK-207 were generously provided by Eukarion Inc. (now Proteome Systems Ltd, Woburn, MA, USA). U0126 was purchased from Tocris Bioscience (Ellisville, MO, USA). Antibodies were obtained from Cell Signaling Technology Inc. (Danvers, MA, USA). All other chemicals used were purchased from Sigma Chemical Co. (St Louis, MO, USA), unless indicated otherwise.

Hippocampal slice preparation

Hippocampi were rapidly dissected from postnatal day 10 or 2-month old Sprague–Dawley rats, and submerged in chilled cutting medium containing 220 mmol/L sucrose, 20 mmol/L NaCl, 2.5 mmol/l KCl, 1.25 mmol/L NaH_2PO_4, 26 mmol/L $NaHCO_3$, 10 mmol/L glucose, 2 mmol/L $MgSO_4$ saturated with 95% O_2–5% CO_2; transverse slices (400 μm thick) were prepared with a McIlwain tissue chopper and placed in incubation baskets in an artificial cerebrospinal fluid (aCSF) containing 124 mmol/L NaCl, 2.5 mmol/L KCl, 1.25 mmol/L KH_2PO_4, 26 mmol/L $NaHCO_3$, 10 mmol/L glucose, 1.5 mmol/L $MgSO_4$, 2.5 mmol/L $CaCl_2$ saturated with 95% O_2–5% CO_2 and incubated for a 1 h-recovery period at 37°C.

Oxygen and glucose deprivation followed by reoxygenation

After 1 h recovery, hippocampal slices in control groups were washed twice with fresh aCSF solution and transferred into individual vials containing 1.5 mL aCSF solution, saturated with 95% O_2–5% CO_2. When hippocampal slices were treated with drugs dissolved in dimethylsulfoxide, dimethylsulfoxide was also added to the control group at the same final concentration as used for the drugs (0.05%). Hippocampal slices in OGD groups were washed twice with an OGD solution containing 124 mmol/L NaCl, 2.5 mmol/L KCl, 1.25 mmol/L KH_2PO_4, 26 mmol/L $NaHCO_3$, 1.5 mmol/L $MgSO_4$, 2.5 mmol/L $CaCl_2$ (pH 7.4), and then transferred into individual vials in 1.5 mL OGD solution, saturated with 95% N_2–5% CO_2. Hippocampal slices were incubated in OGD solution at 34°C for 2 h in anaerobic vials saturated with 95% N_2–5% CO_2. At the end of the OGD period, slices were further incubated for 2.5 h in 1.5 mL fresh aCSF solution saturated with 95% O_2–5% CO_2.

Western blots

Hippocampal slices were homogenized on ice in a lysis buffer containing 150 mmol/L NaCl, 5 mmol/L EDTA, 1% Triton X-100, 10 mmol/L Tris–HCl (pH 7.4), 0.5 mmol/L phenylmethylsulphonyl fluoride, 1 mmol/L sodium orthovanadate, and 1 : 200 protease inhibitor cocktail (Sigma). After sample preparation, 5 or 30 μg total proteins were loaded to each lane of 6% or 8% SDS-PAGE gels and, after separation, proteins were transferred onto polyvinylidene difluoride membranes. The polyvinylidene difluoride membranes were blocked with 5% non-fat milk at 22°C–25°C for 1 h and probed with different primary antibodies (spectrin, 1 : 10 000 dilution; pERK and ERK antibodies, 1 : 1000 dilution; p-p38 and p38 antibodies, 1 : 1000 dilution; pJNK and JNK antibodies, 1 : 2000 dilution) at 4°C overnight. Membranes were then incubated with secondary antibodies for 1 h and developed with ECL solutions. Western blots were scanned and analyzed quantitatively by densitometry with ImageJ software. Levels of phosphorylated proteins were normalized to levels of the respective total proteins.

Cell viability assay

Neuronal damage was assessed by measurement of lactate dehydrogenase (LDH) released into the incubation solution. At the end of the various treatments, 0.3 mL of medium solution was mixed with 0.7 mL potassium phosphate buffer (100 mmol/L K_2HPO_4, adjusted to pH 7.5 with KH_2PO_4). After 20 min, 0.5 mL freshly made sodium pyruvate and NADH solutions were added to this solution immediately followed by measuring absorbance at 340 nm. LDH release was normalized to the corresponding protein concentration in the slices and results are shown as fold of controls. Neuronal damage was also assessed by propidium iodide (PI) uptake. PI (4 μg/mL) was added to the incubation medium at the beginning of treatment, and PI uptake at the indicated times after treatment in hippocampal subfields CA1, CA3, and DG was visualized using a 10X objective with a LSM 510 META inverted microscope fitted with a laser confocal system (Zeiss, Thornwood, NY, USA). Excitation was set at 543 nm and emission was detected with a 560 nm long-pass filter. For each slice, the exact location of the slice surface was determined with the addition of microbeads (Invitrogen, Carlsbad, CA, USA) and by moving the stage up and down until the layer with the brightest fluorescent intensity was found. Images of CA1, CA3, or DG 60 μm below surface were then acquired and analyzed. Fluorescence intensity of confocal images was estimated by the following method: first, images were adjusted to gray levels and captured with Adobe Photoshop, with the background of images in white and PI-stained structures in black; second, modified images were analyzed quantitatively by densitometry with ImageJ software. Finally, data were normalized to the average value found in control slices for each experiment.

ATP measurement

ATP levels were determined by the luciferin-luciferase luminescent reaction using the method described by Rieger (1997). The ATP assay kit was purchased from Sigma (FL-ASC). After treatment, hippocampal slices were homogenized and then centrifuged at 12 000 *g* for 5 min. The supernatant was collected and processed following the kit instructions. Luminescence produced by the luciferin-luciferase reaction was recorded with a scintillation counter. ATP levels were normalized to protein concentration and expressed as nanomole ATP per milligram protein.

Evaluation of ROS production in slices

Levels of ROS production in slices were determined with the fluorescent probe 2′,7′-dichlorofluorescin diacetate (DCFH-DA). A 10 mmol/L DCFH-DA stock solution was prepared and stored at −20°C. Hippocampal slices were subjected to OGD for 2 h in the absence or presence of EUK-189 or EUK-207, and after 1.5 h reoxygenation, they were incubated with 10 μmol/L DCFH-DA for 1 h and then washed twice with PBS. Fluorescent images were obtained with a 5X objective from a microscope fitted with fluorescence detection, and captured with a CCD camera; at this magnification, one image was sufficient to analyze an entire hippocampal slice. Fluorescence intensity was estimated by the same method as for PI uptake described above.

Statistical analysis

Data were generally calculated as fold of control and expressed as means ± SEM from the indicated number of independent experiments. One-way ANOVA with Tukey's *post hoc* test was used to analyze the effects of EUK-189 and EUK-207 on OGD-induced LDH release and PI uptake, and student's *t*-test was used for statistical analyses of other results. *p*-values < 0.05 were considered as statistically significant.

Results

EUK-189 and EUK-207 attenuate OGD-induced cell death in acute hippocampal slices from 2-month-old rats

Acute hippocampal slices from 2-month-old rats were subjected to OGD for 2 h, in the absence or presence of EUK-189 (50 μmol/L) or EUK-207 (50 μmol/L), and LDH release was measured at the end of treatment. OGD treatment induced a 4.13 ± 0.26-fold increase in LDH release, which was partly blocked by EUK-189 (3.21 ± 0.20) and EUK-207 (2.93 ± 0.21, Fig. 1a). At the end of 2 h OGD treatment, hippocampal slices were transferred to fresh aCSF solution and further incubated for 2.5 h in the absence or presence of EUK-189 or EUK-207, saturated with 95% O_2–5% CO_2. LDH release was measured at the end of this recovery period. Compared to control, OGD/reoxygenation treatment induced a 7.33 ± 0.46-fold increase in LDH release, which was again significantly blocked by EUK-189 (5.80 ± 0.32) and EUK-207 (3.85 ± 0.24, Fig. 1b). When hippocampal slices were first subjected to OGD for 2 h, and then transferred to fresh aCSF and incubated for 2.5 h in the absence or presence of EUK-189 or EUK-207 (EUK-189 or EUK-207 applied only during the 2.5 h reoxygenation period), only EUK-207 significantly reduced OGD-induced LDH release (4.90 ± 0.41 vs 7.33 ± 0.46, Fig. 1c).

The neuroprotective effects of EUK-189 and EUK-207 against OGD-induced cell death were also determined by analyzing propidium iodide (PI) uptake in CA1, CA3, and DG regions 60 μm below surface (selection of this level was based on analysis of PI uptake in control slices; the upper layers exhibited intense PI staining as a result of neuronal damage produced during slice preparation) (Fig. 2). Hippocampal slices were treated with OGD for 2 h followed by 2.5 h reoxygenation, in the absence or presence of EUK-189 (50 μmol/L) or EUK-207 (50 μmol/L) throughout the incubation. Compared to control, OGD treatment induced a significant increase in PI staining in the pyramidal layers of CA1 (1.81 ± 0.19-fold increase over control values) and CA3 (1.97 ± 0.17-fold increase over control values), and in the granular layer of DG (1.56 ± 0.14-fold increase over control values). EUK-189 partly decreased PI uptake (1.35 ± 0.21 in CA1, 1.51 ± 0.11 in CA3, and 1.26 ± 0.17 in DG, when compared to control values), while EUK-207 completely reversed OGD-induced PI uptake (0.97 ± 0.11 in CA1, 1.13 ± 0.16 in CA3, and 0.92 ± 0.14 in DG, when compared to control values). One-way ANOVA and Tukey's *post hoc* test indicated that, when compared to EUK-189, EUK-207 provided more protection against OGD-induced neuronal death with both LDH and PI uptake assay.

EUK-189 and EUK-207 partly blocked OGD-induced ATP depletion in acute hippocampal slices

ATP depletion is one of the initial events triggered by ischemia and has been proposed to play a crucial role in cell death. To examine whether treatment with EUK-189 or EUK-207 had any effect on OGD-induced ATP depletion, ATP levels were measured following various experimental treatments. Compared to control, hippocampal slices subjected to OGD for 2 h exhibited ATP levels representing about 25% of control values, an effect that was only slightly changed by treatment with EUK-189 or EUK-207 (Fig. 3a). ATP levels were also measured at the end of the 2.5 h recovery period following the 2 h OGD treatment in the absence or presence of EUK-189 or EUK-207 throughout the incubation. Partial recovery of ATP levels (55% of control values) was observed after 2.5 h reoxygenation under control conditions, and this recovery of ATP levels was further enhanced by treatment with EUK-189 or EUK-207 during the OGD and reoxygenation periods (up to 73% or 76% of control values respectively, an effect which was significantly different from OGD treatment alone (Fig. 3b) On the other hand, when EUK-189 or EUK-207 was applied only

during the 2.5 h reoxygenation period, only small and no significant increases in ATP levels were observed (Fig. 3c).

EUK-189 and EUK-207 completely blocked OGD-induced ROS generation in acute hippocampal slices

To determine whether EUK-189 or EUK-207 protected hippocampal slices from OGD-induced cell death by eliminating free radical formation, ROS accumulation was evaluated with the fluorescent probe DCF. After 2 h OGD treatment followed by 2.5 h reoxygenation in the absence or presence of EUK-189 or EUK-207, DCF fluorescence over the whole hippocampal slices was analyzed with fluorescent microscopy. Compared to untreated control slices, hippocampal slices subjected to OGD exhibited a significant increase in fluorescence intensity (about 156% of control values, Fig. 4); in contrast, slices subjected to OGD in the presence of EUK-189 or EUK-207 exhibited a decrease in DCF fluorescence intensity (86% and 80% of control values, respectively; Fig. 4).

The protective effect of EUK-207 against OGD-induced cell death did not involve the ERK or the p38 pathway

To determine the role of the ERK pathway in our ischemia model, we first determined whether ERK was activated as assessed with measurement of levels of double-phosphorylated ERK1/2 in hippocampal slices subjected to OGD for 2 h followed by 2.5 h reoxygenation (Fig. 5a). Under these conditions, p-ERK1/2 levels were decreased to about 20% of control values. Addition of EUK-189 or EUK-207 in the incubation medium throughout the OGD and reoxygenation periods resulted in a significant recovery of p-ERK1/2 levels to 80% and 50% of control values, respectively (Fig. 5b). When the MEK inhibitor, U0126 (10 μmol/L), was applied alone or together with EUK-189 or EUK-207, it completely blocked ERK1/2 phosphorylation, as expected. However, treatment with U0126 had no effect on OGD-induced LDH release or on the protective effects of EUK-189 and EUK-207 against OGD-induced LDH release (Fig. 5c and d).

We previously reported that the mechanisms underlying OGD-induced cell death were different in slices prepared from neonatal as compared to adult rats (Zhou and Baudry 2006). We therefore tested the roles of ROS and of ERK on OGD-induced cell death in slices from neonatal rats. In contrast to the striking OGD-induced decrease in ERK phosphorylation in slices from adult rats, slices prepared from postnatal day 10 rats and subjected to OGD for 2 h followed by 2.5 h reoxygenation showed a slight increase in ERK1/2 phosphorylation (Fig. 6a and b). OGD-induced LDH release was also significantly reduced by EUK-207 (Fig. 6c). Treatment with EUK-207 did not modify ERK1/2 phosphorylation levels when compared to either control or OGD. As observed in slices from adult rats, U0126 completely blocked ERK1/2 activation when applied alone or together with EUK-207 (Fig. 6a and b), and also had no effect on OGD-induced LDH release either by itself or in the presence of EUK-207 (Fig. 6c).

To determine the roles of p38 and JNK pathways in the neuroprotective effects of EUK-207, we tested the levels of phosphorylated p38 and JNK. Acute hippocampal slices from 2-month-old and postnatal day 10 rats were subjected to OGD for 2 h followed by 2.5 h reoxygenation (Fig. 7). Under these conditions, p-p38 levels were slightly decreased to 81% of control values ($p > 0.05$, *t*-test) in slices from postnatal day 10 rats and decreased to 60% of control values ($p < 0.05$, *t*-test) in slices from 2-month-old rats (Fig. 7a and b). ANOVA with Tukey's *post hoc* test indicated that in slices from either 2-month-old or postnatal day 10 rats, there were no significant differences between any group of treatment when slices were subjected to OGD in the absence or presence of EUK-207 (50 μmol/L), EUK-207 plus PD98059 (MEK1/2 inhibitor, 10 μmol/L), or EUK-207 plus SB203580 (p38 inhibitor, 1

μmol/L). When slices were subjected to OGD for 2 h followed by 2.5 h reoxygenation, p-JNK levels were significantly decreased to below 20% of control values ($p < 0.05$, *t*-test) in slices from both 2-month-old and postnatal day 10 rats (Fig. 7c and d). ANOVA with Tukey's *post hoc* test indicated that there were no significant differences between any treatment in slices from both ages either. When hippocampal slices from 2-month-old and postnatal day 10 rats were subjected to 2 h OGD w/o reoxygenation, or 2 h OGD followed by 2.5 h reoxygenation, PD98059 or SB203580 did not modify OGD-induced LDH release or the protective effects of EUK-207 against OGD-induced LDH release when applied alone or together with EUK-207 (Fig. 8).

The neuroprotective effects of EUK-189 and EUK-207 against OGD-induced cell death did not involve blockade of calpain activation

We previously reported that acute hippocampal slices from postnatal day 7 or adult rats subjected to OGD followed by reoxygenation exhibited calpain activation as evidenced by increased levels of calpain-mediated spectrin breakdown products (SBDPs) with an apparent molecular weight of 145–150 kD (Zhou and Baudry 2006). However, when slices were treated with EUK-189 or EUK-207 during the OGD and reoxygenation periods, no significant changes in SBDPs were observed compared to OGD alone (Fig. 9).

Discussion

Our results indicate that, among the multiple pathways activated as a result of ischemia/reperfusion, excessive production of reactive oxygen species represents a critical step in the rapid phase of neurodegeneration observed in both neonatal and adult hippocampal slices. On the other hand, ERK, p38, JNK and calpain activation do not seem to play a major role in this initial phase of neuronal death, although calpain activation does play some role in neonatal rats (Zhou and Baudry 2006). OGD has been shown to elicit rapid decrease in ATP levels, increased intracellular calcium concentration, release of glutamate followed by overactivation of glutamate receptors, excessive generation of ROS, mitochondria dysfunction, and ultimately cell death by both necrosis- and apoptosis-mediated cell death (reviewed in Koistinaho and Koistinaho 2005; Zipp and Aktas 2006; Won *et al.* 2002). The exact temporal sequence of events and the relative importance of these different events remain far from being understood. Our results indicate that increased formation of reactive oxygen species might take place relatively early in this sequence, possibly even before reoxygenation occurs, as the two synthetic superoxide dismutase/catalase mimetics, EUK-189 and EUK-207, produced better neuroprotection when applied at the beginning of the OGD period than only during the reoxygenation period.

In his comprehensive 1999 review, P. Lipton proposed a sequence of events comprising initiators and activators followed by perpetrators leading from the initial ischemic insults to cell death (Lipton 1999). Accordingly, the loss of ATP initiates membrane depolarization, glutamate release, and increased intracellular calcium. Ischemia also induced gene activation possibly mediated through MAP kinase activation, as well as increased production of oxygen free radicals and peroxynitrite. These events are followed by activation of proteases, including calpain, mitochondrial dysfunction, prolonged changes in kinases and phosphatases, cytoskeletal damage and cell death. It has also previously been suggested that the degree of ATP depletion determines the form of death cells will exhibit, with gradual ATP depletion after mild ischemia inducing caspase-3 release and apoptosis, while rapid ATP depletion with severe ischemia will elicit extreme cytochrome c release and necrosis (Li *et al.* 1997; Saikumar *et al.* 1998). Drugs that prevent ATP depletion or promote ATP recovery after ischemia have been reported to increase cell survival when applied before, during or after the ischemic insult (Riepe *et al.* 1997; Galeffi *et al.* 2000).

In our model, 2 h OGD treatment decreased ATP levels to about 25% of control, an effect that is not modified by the presence of EUK-189 or EUK-207. Thus, as expected, the neuroprotective effect of these compounds is not the result of prevention of the ATP loss produced by ischemia. The significant degree of ATP recovery observed when EUK-189 or EUK-207 was applied during and after the OGD period, as compared to control, is probably the result of the decrease in cell damage produced by these compounds. ATP depletion can further contribute to the collapse of the mitochondrial membrane potential, the opening of mitochondrial perme-ability transition pore (MPTP), the release of small proteins, such as apoptosis-inducing factor and cytochrome c, and accumulation of free radicals (reviewed by Fiskum *et al.* 1999; Murphy *et al.* 1999). ATP depletion initiates MPTP opening and increases ROS levels, which then in turn potentiate ATP depletion. It is thus expected that the EUK compounds will provide some degree of protection for mitochondria as previously described in the SOD1 null mice (Melov *et al.* 2001).

Our DCF fluorescence results indicated that EUK-189 or EUK-207 completely blocked the formation of ROS elicited by OGD and reoxygenation. These results strongly suggest that the rapid OGD and reoxygenation-induced cell death in acute hippocampal slices is, at least in part, as a result of increased free radical production, and that the neuroprotective effects of EUK-207 and EUK-189 are linked to their ability to eliminate ROS. Although EUK-189 and EUK-207 are both synthetic superoxide dismutase/catalase mimetics with relatively similar structures (Liu *et al.* 2003), our results with LDH release and PI uptake indicated that EUK-207 exhibited better neuroprotective effects than EUK-189. The PI staining results in different hippocampal subfields indicated that PI uptake after OGD/reoxygenation was higher in CA1 and CA3 than in DG, and that only EUK-207 exhibited significant neuroprotection in all three subfields. The difference in neuroprotective effects between EUK-189 and EUK-207 might occur as a result of their structural differences as EUK-207 has similar catalytic activities but greater biological stability than EUK-189 (Liu *et al.* 2003), which might be an important factor in our OGD model in acute hippocampal slices.

MAP Kinase pathways have often been implicated in ischemia-induced cell death, although the role of MEK/ERK pathway remains controversial. It has generally been proposed that MEK/ERK activation is involved both in cell death and neuroprotective/survival effects during ischemia and after reperfusion (Alessandrini *et al.* 1999; Fahlman *et al.* 2002). Some studies have shown that MEK inhibitors, such as U0126 or PD-98059 can reduce cell death induced by seizures, glutamate excitotoxicity, and OGD (Murray *et al.* 1998; Namura *et al.* 2001; Zhu *et al.* 2005); however, recent studies have also shown that inhibition of the MEK/ERK pathway blocked the neuroprotective effects of N-acetyl- O-methyldopamine (NAMDA), or fructose-1,6-bis-phosphate against ischemia/hypoxia (Fahlman *et al.* 2002; Park *et al.* 2004), or had no effect in ischemia-induced cell death (Abe and Saito 2000; Sugino *et al.* 2000a). The dual role of the MEK/ERK pathway may depend on the animal model, or the duration of ERK activation (Park *et al.* 2004). In our experiments, ERK1/2 was inactivated after OGD and reoxygenation in slices from 2-month-old rats, an effect that was partially restored by EUK-189 or EUK-207. The MEK inhibitor U0126 completely blocked ERK1/2 activation whether slices were treated with or without EUK-189 or EUK-207; however, U0126 did not modify OGD-induced cell death, nor did it modify EUK-189- or EUK-207-mediated protection against OGD-induced cell death. Moreover, while OGD and reoxygenation treatment elicited high-LDH release in hippocampal slices prepared from postnatal 10 rats, ERK1/2 activation levels were not affected and U0126 did not modify EUK-207 mediated neuroprotection against OGD-induced cell death under these conditions. Thus, our results clearly indicate that ERK1/2 is not involved in early ischemia-induced cell death. It remains possible though that this pathway participates in more delayed forms of ischemia-induced cell death.

A similar conclusion can be drawn for the other members of the MAP kinase pathways, p38 and JNK. EUK-207 had no effect on OGD-induced slight p38 dephosphorylation and significant JNK dephosphorylation in slices from either 2-month-old or postnatal day 10 rats. Although p38 inhibition has been shown to provide neuronal protection in cerebral ischemia (Sugino *et al.* 2000b; Barone *et al.* 2001), in acute hippocampal slices the p38 inhibitors, SB203580 or SB202190 (data not show), did not modify OGD-induced cell death or EUK-207-mediated neuroprotection against OGD-induced cell death. All these results suggest that the MAP kinase pathways are not involved in OGD-induced cell death and are not involved in the neuroprotective effects of EUK-189 or EUK-207 against the rapid phase of OGD-induced cell death in acute hippocampal slices.

Calpain activation has also been reported to be involved in hypoxia and ischemia, presumably because overactivation of glutamate receptors, and in particular receptors, increases intracellular calcium concentration (Neumar *et al.* 2001; Yamashima *et al.* 2003; Yokota *et al.* 2003). Calpain inhibitors have been shown to reduce neurodegeneration and cell death in different ischemia models both in neonatal and adult animals (Bartus *et al.* 1994; Markgraf *et al.* 1998; Kawamura *et al.* 2005; Khalil *et al.* 2005). Our results indeed showed that spectrin degradation increased after OGD and reoxygenation, indicating that calpain was activated following OGD/reoxygenation in hippocampal slices from both neonatal and adult rats. However, this effect was not modified following treatment with EUK-189 or EUK-207. This result suggests that, although calpain might play an important role in ischemia-induced neuropathology, the neuroprotective effects of EUK-189 or EUK-207 is not the result of inhibition of calpain activation. As mentioned above, ATP depletion induces glutamate release and increased intracellular calcium concentration resulting in stimulation of the calcium-dependent protease, calpain. Our results suggest that calcium influx and calpain activation might precede free radical production; alternatively, these 2 sets of events are unrelated and calpain activation might participate in delayed forms of ischemia-induced neuronal death.

We previously reported data indicating that the mechanisms underlying OGD-induced cell death were different in slices from neonatal and adult rats (Zhou and Baudry 2006), and our present results further confirm this interpretation. In the present experiments, OGD/reoxygenation in neonatal slices was not associated with decreased levels in ERK1/2, in contrast to what was observed in slices prepared from adult rats. This effect could be related to the much lower decrease in ATP levels resulting from OGD in slices from neonatal compared to adult slices (data not shown), an effect possibly correlated to the anaerobic nature of metabolism in neonatal animals (Bickler *et al.* 1993; Folbergrova 1993).

In conclusion, our data indicate that like many salen-manganese complexes that are neuroprotective in various models of neurological diseases, EUK-189 and EUK-207 provide significant protection against rapid OGD-induced cell death in acute hippocampal slices, by eliminating free radicals generation, but not through the MAP kinase pathways or attenuation of calpain activation. While our results also document the critical roles of oxygen free radicals in rapid ischemia-induced neuronal death, they stress the needs for further studies to better understand the links between early events set up by ischemic insults and delayed forms of ischemia-induced cell death.

Acknowledgments

This work was supported by Grants AG-14751 from the NIA (PI: Dr, C. Finch) and NS048521-02 from NINDS (MB).

Abbreviations used

DCF	dichlorofluorescin
ERK	extracellular signal- regulated kinase
JNK	Jun N-terminal kinase
MAPK	mitogen-activated protein kinases
ROS	reactive oxygen species

References

Abe K, Saito H. Amyloid beta neurotoxicity not mediated by the mitogen-activated protein kinase cascade in cultured rat hippocampal and cortical neurons. Neurosci Lett. 2000; 292:1–4. [PubMed: 10996435]

Al Majed AA, Sayed-Ahmed MM, Al Omar FA, Al Yahya AA, Aleisa AM, Al Shabanah OA. Carnitine esters prevent oxidative stress damage and energy depletion following transient forebrain ischaemia in the rat hippocampus. Clin Exp Pharmacol Physiol. 2006; 33:725–733. [PubMed: 16895547]

Alessandrini A, Namura S, Moskowitz MA, Bonventre JV. MEK1 protein kinase inhibition protects against damage resulting from focal cerebral ischemia. Proc Natl Acad Sci USA. 1999; 96:12866–12869. [PubMed: 10536014]

Baker K, Marcus CB, Huffman K, Kruk H, Malfroy B, Doctrow SR. Synthetic combined superoxide dismutase/catalase mimetics are protective as a delayed treatment in a rat stroke model: a key role for reactive oxygen species in ischemic brain injury. J Pharmacol Exp Ther. 1998; 284:215–221. [PubMed: 9435181]

Barone FC, Irving EA, Ray AM, et al. Inhibition of p38 mitogen-activated protein kinase provides neuroprotection in cerebral focal ischemia. Med Res Rev. 2001; 21:129–145. [PubMed: 11223862]

Bartus RT, Baker KL, Heiser AD, Sawyer SD, Dean RL, Elliott PJ, Straub JA. Postischemic administration of AK275, a calpain inhibitor, provides substantial protection against focal ischemic brain damage. J Cereb Blood Flow Metab. 1994; 14:537–544. [PubMed: 8014200]

Bickler PE, Gallego SM, Hansen BM. Developmental changes in intracellular calcium regulation in rat cerebral cortex during hypoxia. J Cereb Blood Flow Metab. 1993; 13:811–819. [PubMed: 8103057]

Claytor RB, Aranson NJ, Ignotz RA, Lalikos JF, Dunn RM. Remote ischemic preconditioning modulates p38 MAP kinase in rat adipocutaneous flaps. J Reconstr Microsurg. 2007; 23:93–98. [PubMed: 17330205]

Doctrow SR, Huffman K, Marcus CB, et al. Salen-manganese complexes as catalytic scavengers of hydrogen peroxide and cytoprotective agents: structure-activity relationship studies. J Med Chem. 2002; 45:4549–4558. [PubMed: 12238934]

Doctrow, SR.; Adinolfi, C.; Baudry, M., et al. Salen manganese complexes, combined superoxide dismutase/catalase mimetics demonstrate potential for treating neurodegenerative and other ageassociated disease. In: Rodriguez, H.; Cutler, R., editors. Oxidative Stress and Aging: Advances in Basic Science, Diagnostics, and Intervention. World Scientific Publishing Company; Hackensack, NJ, USA: 2003. p. 1324-1343.

Fahlman CS, Bickler PE, Sullivan B, Gregory GA. Activation of the neuroprotective ERK signaling pathway by fructose-1,6-bisphosphate during hypoxia involves intracellular Ca2+ and phospholipase C. Brain Res. 2002; 958:43–51. [PubMed: 12468029]

Fiskum G, Murphy AN, Beal MF. Mitochondria in neurodegeneration: acute ischemia and chronic neurodegenerative diseases. J Cereb Blood Flow Metab. 1999; 19:351–369. [PubMed: 10197505]

Folbergrova J. Cerebral energy state of neonatal rats during seizures induced by homocysteine. Physiol Res. 1993; 42:155–160.

Galeffi F, Sinnar S, Schwartz-Bloom RD. Diazepam promotes ATP recovery and prevents cytochrome c release in hippocampal slices after *in vitro* ischemia. J Neurochem. 2000; 75:1242–1249. [PubMed: 10936207]

Gupta S, Sharma SS. Neuroprotective effects of trolox in global cerebral ischemia in gerbils. Biol Pharm Bull. 2006; 29:957–961. [PubMed: 16651726]

Karadottir R, Cavelier P, Bergersen LH, Attwell D. NMDA receptors are expressed in oligodendrocytes and activated in ischaemia. Nature. 2005; 438:1162–1166. [PubMed: 16372011]

Kawamura M, Nakajima W, Ishida A, Ohmura A, Miura S, Takada G. Calpain inhibitor MDL 28170 protects hypoxicischemic brain injury in neonatal rats by inhibition of both apoptosis and necrosis. Brain Res. 2005; 1037:59–69. [PubMed: 15777753]

Kelly BL, Ferreira A. Beta-amyloid-induced dynamin 1 degradation is mediated by NMDA receptors in hippocampal neurons. J Biol Chem. 2006; 281:28079–28089. [PubMed: 16864575]

Khalil PN, Neuhof C, Huss R, Pollhammer M, Khalil MN, Neuhof H, Fritz H, Siebeck M. Calpain inhibition reduces infarct size and improves global hemodynamics and left ventricular contractility in a porcine myocardial ischemia/reperfusion model. Eur J Pharmacol. 2005; 528:124–131. [PubMed: 16324693]

Koistinaho M, Koistinaho J. Interactions between Alzheimer's disease and cerebral ischemia–focus on inflammation. Brain Res Brain Res Rev. 2005; 48:240–250. [PubMed: 15850663]

Kovacs K, Toth A, Deres P, Kalai T, Hideg K, Gallyas F Jr, Sumegi B. Critical role of PI3-kinase/Akt activation in the PARP inhibitor induced heart function recovery during ischemia-reperfusion. Biochem Pharmacol. 2006; 71:441–452. [PubMed: 16337154]

Li P, Nijhawan D, Budihardjo I, Srinivasula SM, Ahmad M, Alnemri ES, Wang X. Cytochrome c and dATP-dependent formation of Apaf-1/caspase-9 complex initiates an apoptotic protease cascade. Cell. 1997; 91:479–489. [PubMed: 9390557]

Lin CH, Kuo SC, Huang LJ, Gean PW. Neuroprotective effect of N-acetylcysteine on neuronal apoptosis induced by a synthetic gingerdione compound: involvement of ERK and p38 phosphorylation. J Neurosci Res. 2006; 84:1485–1494. [PubMed: 16983658]

Lipton P. Ischemic cell death in brain neurons. Physiol Rev. 1999; 79:1431–1568. [PubMed: 10508238]

Liu R, Liu IY, Bi X, Thompson RF, Doctrow SR, Malfroy B, Baudry M. Reversal of age-related learning deficits and brain oxidative stress in mice with superoxide dismutase/catalase mimetics. Proc Natl Acad Sci USA. 2003; 100:8526–8531. [PubMed: 12815103]

Lynch G, Baudry M. Brain spectrin, calpain and long-term changes in synaptic efficacy. Brain Res Bull. 1987; 18:809–815. [PubMed: 3040193]

Markgraf CG, Velayo NL, Johnson MP, McCarty DR, Medhi S, Koehl JR, Chmielewski PA, Linnik MD. Six-hour window of opportunity for calpain inhibition in focal cerebral ischemia in rats. Stroke. 1998; 29:152–158. [PubMed: 9445345]

Melov S, Ravenscroft J, Malik S, Gill MS, Walker DW, Clayton PE, Wallace DC, Malfroy B, Doctrow SR, Lithgow GJ. Extension of life-span with superoxide dismutase/catalase mimetics. Science. 2000; 289:1567–1569. [PubMed: 10968795]

Melov S, Doctrow SR, Schneider JA, Haberson J, Patel M, Coskun PE, Huffman K, Wallace DC, Malfroy B. Lifespan extension and rescue of spongiform encephalopathy in superoxide dismutase 2 nullizygous mice treated with superoxide dismutasecatalase mimetics. J Neurosci. 2001; 21:8348–8353. [PubMed: 11606622]

Murphy AN, Fiskum G, Beal MF. Mitochondria in neurodegeneration: bioenergetic function in cell life and death. J Cereb Blood Flow Metab. 1999; 19:231–245. [PubMed: 10078875]

Murray B, Alessandrini A, Cole AJ, Yee AG, Furshpan EJ. Inhibition of the p44/42 MAP kinase pathway protects hippocampal neurons in a cell-culture model of seizure activity. Proc Natl Acad Sci USA. 1998; 95:11975–11980. [PubMed: 9751775]

Musleh W, Bruce A, Malfroy B, Baudry M. Effects of EUK-8, a synthetic catalytic superoxide scavenger, on hypoxiaand acidosis-induced damage in hippocampal slices. Neuropharmacology. 1994; 33:929–934. [PubMed: 7969813]

Namura S, Iihara K, Takami S, Nagata I, Kikuchi H, Matsushita K, Moskowitz MA, Bonventre JV, Alessandrini A. Intravenous administration of MEK inhibitor U0126 affords brain protection against forebrain ischemia and focal cerebral ischemia. Proc Natl Acad Sci USA. 2001; 98:11569–11574. [PubMed: 11504919]

Neumar RW, Meng FH, Mills AM, Xu YA, Zhang C, Welsh FA, Siman R. Calpain activity in the rat brain after transient forebrain ischemia. Exp Neurol. 2001; 170:27–35. [PubMed: 11421581]

Park EM, Joh TH, Volpe BT, Chu CK, Song G, Cho S. A neuroprotective role of extracellular signal-regulated kinase in N-acetyl-O-methyldopamine-treated hippocampal neurons after exposure to *in vitro* and *in vivo* ischemia. Neuroscience. 2004; 123:147–154. [PubMed: 14667449]

Peng J, Stevenson FF, Doctrow SR, Andersen JK. Superoxide dismutase/catalase mimetics are neuroprotective against selective paraquat-mediated dopaminergic neuron death in the substantial nigra: implications for Parkinson disease. J Biol Chem. 2005; 280:29194–29198. [PubMed: 15946937]

Pong K, Doctrow SR, Huffman K, Adinolfi CA, Baudry M. Attenuation of staurosporine-induced apoptosis, oxidative stress, and mitochondrial dysfunction by synthetic superoxide dismutase and catalase mimetics, in cultured cortical neurons. Exp Neurol. 2001; 171:84–97. [PubMed: 11520123]

Ray SK, Fidan M, Nowak MW, Wilford GG, Hogan EL, Banik NL. Oxidative stress and Ca2+ influx upregulate calpain and induce apoptosis in PC12 cells. Brain Res. 2000; 852:326–334. [PubMed: 10678759]

Rieger D. Batch analysis of the ATP content of bovine sperm, oocytes, and early embryos using a scintillation counter to measure the chemiluminescence produced by the luciferin-luciferase reaction. Anal Biochem. 1997; 246:67–70. [PubMed: 9056184]

Riepe MW, Kasischke K, Raupach A. Acetylsalicylic acid increases tolerance against hypoxic and chemical hypoxia. Stroke. 1997; 28:2006–2011. [PubMed: 9341711]

Rong Y, Doctrow SR, Tocco G, Baudry M. EUK-134, a synthetic superoxide dismutase and catalase mimetic, prevents oxidative stress and attenuates kainate-induced neuropathology. Proc Natl Acad Sci USA. 1999; 96:9897–9902. [PubMed: 10449791]

Saikumar P, Dong Z, Weinberg JM, Venkatachalam MA. Mechanisms of cell death in hypoxia/reoxygenation injury. Oncogene. 1998; 17:3341–3349. [PubMed: 9916996]

Sugino T, Nozaki K, Takagi Y, Hattori I, Hashimoto N, Moriguchi T, Nishida E. Activation of mitogen-activated protein kinases after transient forebrain ischemia in gerbil hippocampus. J Neurosci. 2000a; 20:4506–4514. [PubMed: 10844020]

Wang X, Wang H, Xu L, Rozanski DJ, Sugawara T, Chan PH, Trzaskos JM, Feuerstein GZ. Significant neuroprotection against ischemic brain injury by inhibition of the MEK1 protein kinase in mice: exploration of potential mechanism associated with apoptosis. J Pharmacol Exp Ther. 2003; 304:172–178. [PubMed: 12490588]

Won SJ, Kim DY, Gwag BJ. Cellular and molecular pathways of ischemic neuronal death. J Biochem Mol Biol. 2002; 35:67–86. [PubMed: 16248972]

Yamashima T, Tonchev AB, Tsukada T, Saido TC, Imajoh-Ohmi S, Momoi T, Kominami E. Sustained calpain activation associated with lysosomal rupture executes necrosis of the postischemic CA1 neurons in primates. Hippocampus. 2003; 13:791–800. [PubMed: 14620874]

Yokota M, Saido TC, Kamitani H, Tabuchi S, Satokata I, Watanabe T. Calpain induces proteolysis of neuronal cyto-skeleton in ischemic gerbil forebrain. Brain Res. 2003; 984:122–132. [PubMed: 12932846]

Zhou M, Baudry M. Developmental changes in NMDA neurotoxicity reflect developmental changes in subunit composition of NMDA receptors. J Neurosci. 2006; 26:2956–2963. [PubMed: 16540573]

Zhu D, Wu X, Strauss KI, Lipsky RH, Qureshi Z, Terhakopian A, Novelli A, Banaudha K, Marini AM. N-methyl-D-aspartate and TrkB receptors protect neurons against glutamate excitotoxicity through an extracellular signal-regulated kinase pathway. J Neurosci Res. 2005; 80:104–113. [PubMed: 15744743]

Zipp F, Aktas O. The brain as a target of inflammation: common pathways link inflammatory and neurodegenerative diseases. Trends Neurosci. 2006; 29:518–527. [PubMed: 16879881]

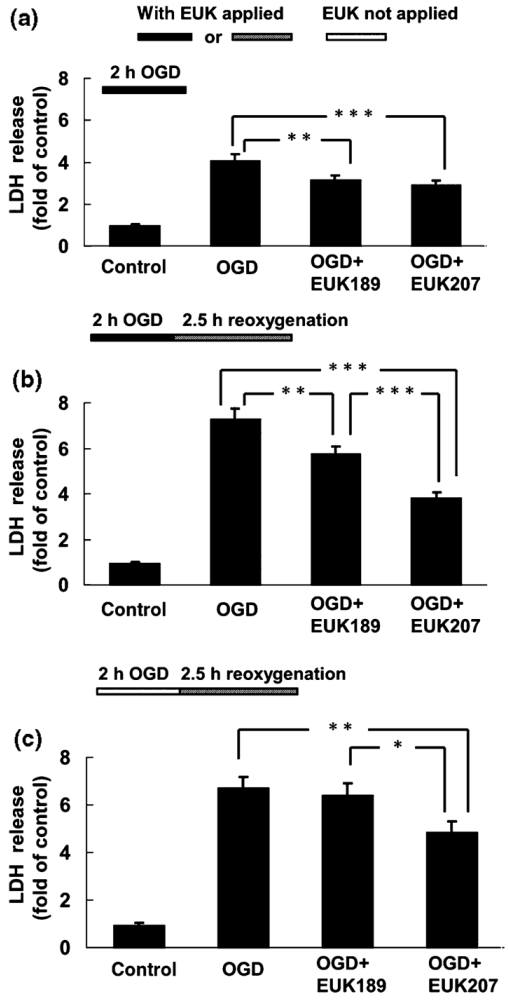

Fig. 1.

Effects of EUK-189 and EUK-207 on OGD-induced LDH release in acute hippocampal slices from 2-month-old rats. (a) Hippocampal slices were subjected to OGD for 2 h in the absence or presence of EUK-189 (50 μmol/L) or EUK-207 (50 μmol/L). LDH release was measured at the end of 2 h OGD treatment. Results are expressed as fold increase over control values and are means ± SEM of 25 experiments. (b) Hippocampal slices were subjected to OGD for 2 h followed by 2.5 h reoxygenation (in fresh aCSF in the presence of normal O_2/CO_2 conditions), in the absence or presence of EUK-189 or EUK-207 throughout the treatment. LDH release was measured at the end of the 2.5 h reoxygenation treatment. Results are means ± SEM of 30 experiments. (c) All hippocampal slices were subjected to OGD for 2 h, transferred to fresh aCSF and treated for 2.5 h in the absence or presence of EUK-189 or EUK-207 (with EUK-189 or EUK-207 applied only during the 2.5 h reoxygenation). LDH release was measured at the end of the 2.5 h treatment. Results are means ± SEM of eight experiments. Statistical analysis was carried out by one-way ANOVA followed by Tukey's *post hoc* test (*$p < 0.05$, **$p < 0.01$, ***$p < 0.001$).

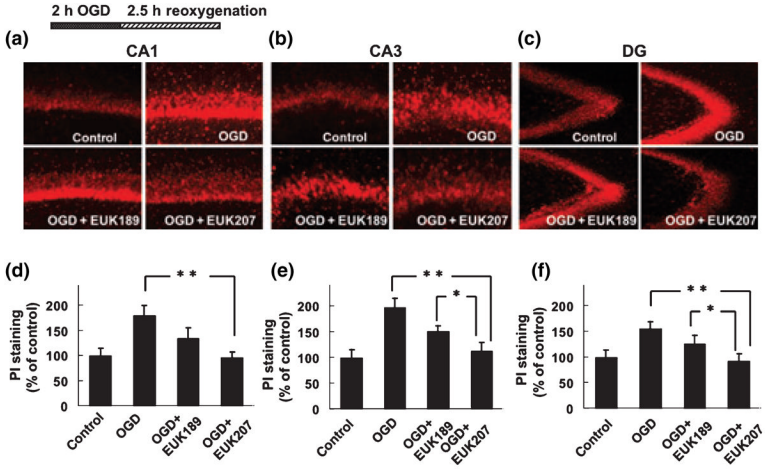

Fig. 2.

Effects of EUK-189 and EUK-207 on OGD-induced increase in PI uptake in different regions of acute hippocampal slices from 2-month-old rats. Hippocampal slices were subjected to OGD for 2 h followed by 2.5 h reoxygenation in the absence or presence of EUK- 189 (50 μmol/L) or EUK-207 (50 μmol/L). Representative images of PI staining in CA1 region (a), CA3 region (b), or DG region (c) 60 μm below the surface of acute hippocampal slices are displayed (d and e), and (f) Quantification of PI staining in different hippocampal subfields (d: CA1; e: CA3; f: DG). PI staining intensity was analyzed as described under Materials and methods. Results are expressed as percent of control values and are means ± SEM of 11 experiments. Statistical analysis was carried out by one-way ANOVA followed by Tukey's *post hoc* test (*$p < 0.05$, **p 0.01).

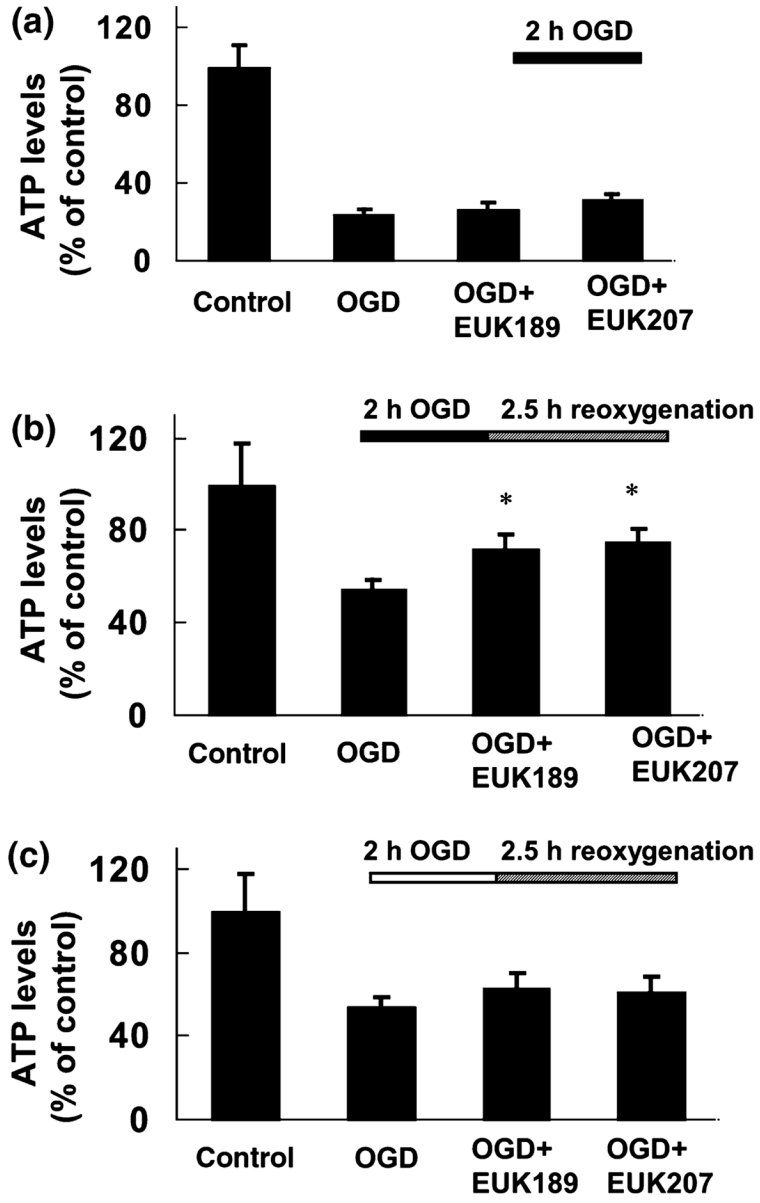

Fig. 3.

Effects of EUK-189 and EUK-207 on OGD-induced ATP depletion in acute hippocampal slices from 2-month-old rats. (a) Hippocampal slices were subjected to OGD for 2 h in the absence or presence of EUK-189 (50 μmol/L) or EUK-207 (50 μmol/L). ATP levels were measured at the end of the 2 h OGD treatment. (b) Hippocampal slices were subjected to OGD for 2 h followed by 2.5 h reoxygenation in the absence or presence of EUK-189 or EUK-207. ATP levels were measured at the end of the 2.5 h reoxygenation treatment. (c) All hippocampal slices were subjected to OGD for 2 h. They were then transferred to fresh aCSF and treated for 2.5 h in the absence or presence of EUK-189 or EUK-207 (with EUK-189 or EUK-207 applied only during the 2.5 h reoxygenation period). ATP levels were measured at the end of treatment. Results are expressed as percent decrease over the respective control values and are means ± SEM of five experiments. Statistical analysis was performed by student's *t*-test (*$p < 0.05$ as compared to OGD-treated slices).

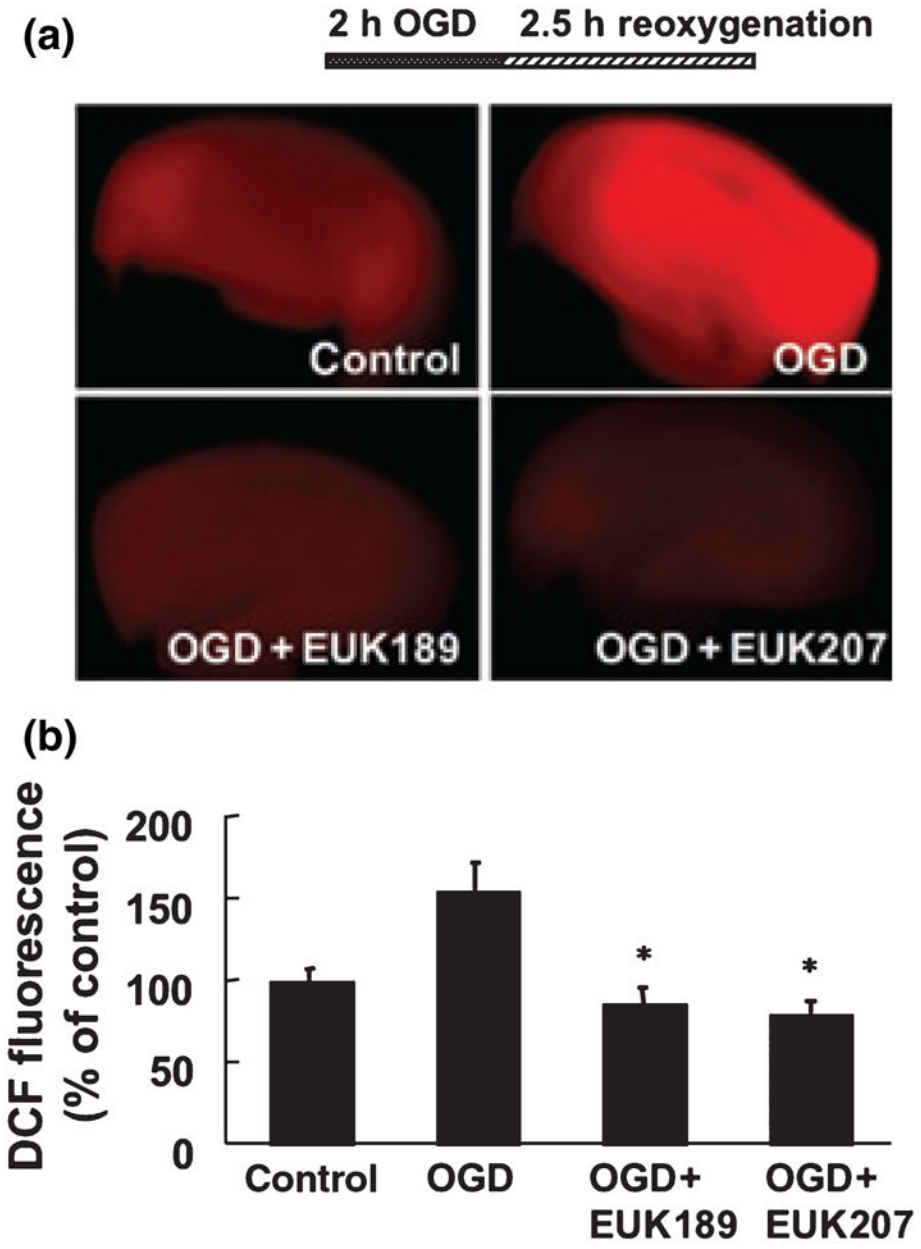

Fig. 4.

Effects of EUK-189 and EUK-207 on OGD-induced ROS generation in acute hippocampal slices from 2-month-old rats. Hippocampal slices were subjected to OGD for 2 h followed by 1.5 h reoxygenation in the absence or presence of EUK-189 (50 μmol/L) or EUK-207 (50 μmol/L). DCFH-DA (10 μmol/L) was then added for another 1 h-period of reoxygenation. (a) Representative images of DCF fluorescence in whole hippocampal slices subjected to OGD for 2 h followed by 2.5 h reoxygenation in the absence or presence of EUK-189 or EUK-207. (b) Quantification of DCF fluorescence intensity. Results are expressed as percent of control values and are means ± SEM of 15 experiments. (*$p < 0.05$ as compared to OGDtreated slices, student's *t*-test).

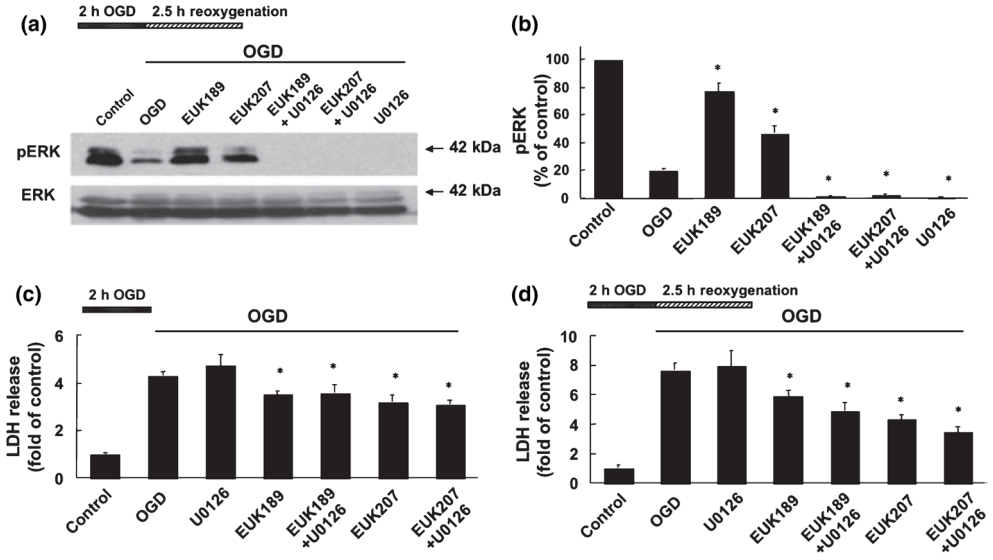

Fig. 5.

Effects of U0126, EUK-189, or EUK-207 on OGD-induced changes in ERK1/2 phosphorylation, and on OGD-induced LDH release in acute hippocampal slices from 2-month-old rats. Acute hippocampal slices were subjected to OGD for 2 h followed by 2.5 h reoxygenation. At the end of incubation, slices were homogenized and aliquots were processed for immunoblotting with antibodies against double-phosphorylated ERK (pERK) and total ERK. (a) Representative images of western blots indicating the pERK and ERK levels at 42 and 44 kDa in the absence or presence of EUK-189 (50 μmol/L), EUK-207 (50 μmol/L), EUK-189 plus U0126, EUK-207 plus U0126, or U0126 (10 μmol/L). (b) Quantitative analysis of blots similar to those shown in A. Blots were scanned and the intensities of pERK bands were quantified and normalized to the intensities of ERK bands. Results were expressed as percent of control values and the data represent means ± SEM of five experiments. (c) Hippocampal slices were subjected to OGD for 2 h and LDH release was measured at the end of the 2 h OGD treatment. Results are expressed as fold increase over control values and are means ± SEM of 10 experiments. (d) Hippocampal slices were subjected to OGD for 2 h followed by 2.5 h reoxygenation. LDH release was measured at the end of the 2.5 h reoxygenation treatment. Results are means ± SEM of 10 experiments (*$p < 0.05$ as compared to OGD-treated slices, student's *t*-test).

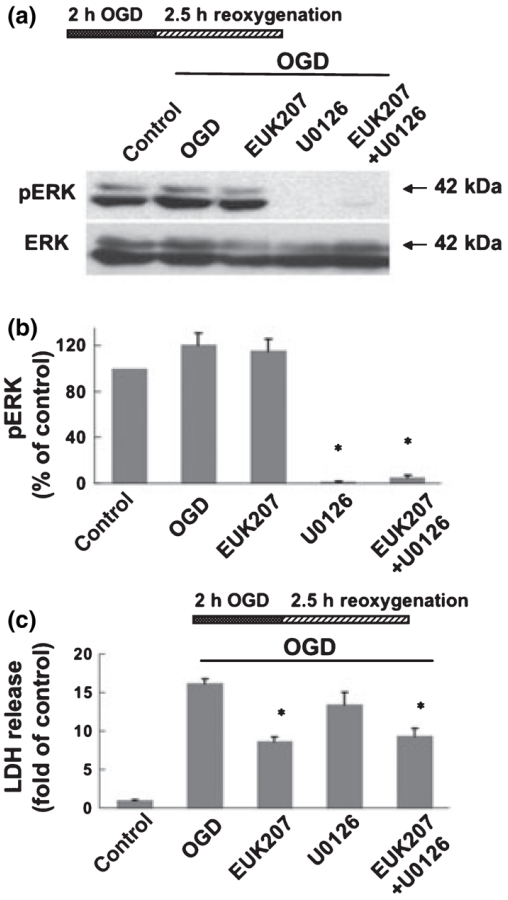

Fig. 6.

Effects of U0126 or EUK-207 on ERK1/2 phosphorylation, and on OGD-induced LDH release in acute hippocampal slices from postnatal day 10 rats. Acute hippocampal slices from postnatal day 10 rats were subjected to OGD for 2 h followed by 2.5 h reoxygenation in the absence or presence of U0126 (10 μmol/L) or EUK-207 (50 μmol/L). At the end of treatment, slices were homogenized and aliquots were processed for immunoblotting with pERK and ERK antibodies. LDH release in medium was measured as an index of toxicity. (a) Representative images of western blots indicating the pERK and ERK levels at 42 and 44 kDa in the absence or presence of EUK-207, U0126, or EUK-207 plus U0126. (b) Quantitative analysis of blots similar to those shown in (a). Blots were scanned and the intensities of pERK bands were quantified and normalized to the intensities of ERK. The results are expressed as percent of control values and the data represent means ± SEM of four experiments. (c) Hippocampal slices were subjected to OGD for 2 h followed by 2.5 h reoxygenation, in the absence or presence of EUK-207, U0126, or EUK-207 plus U0126. LDH release was measured at the end of the 2.5 h reoxygenation treatment. Results are expressed as fold increase over control values and are means ± SEM of 10 experiments (*$p < 0.05$ as compared to OGD-treated slices, student's *t*-test).

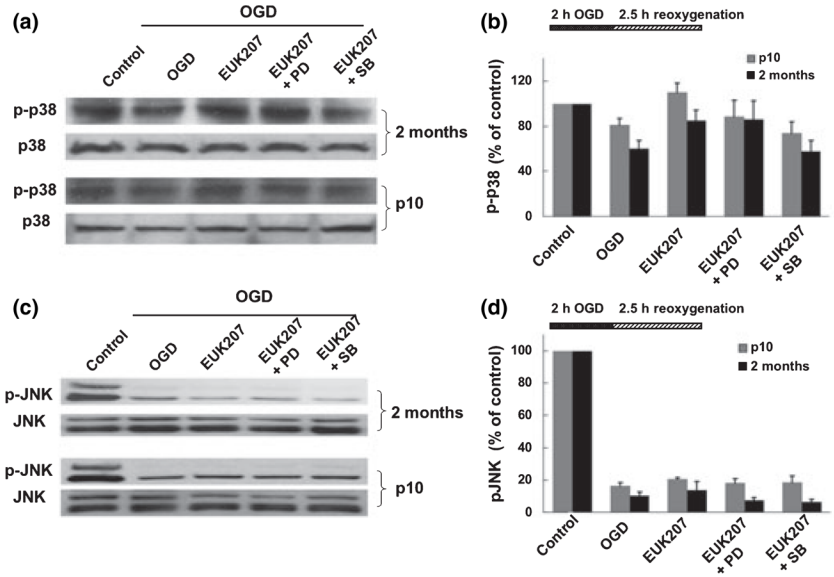

Fig. 7.

Effects of EUK-207 on OGD-induced changes of p38 and JNK phosphorylation in acute hippocampal slices from 2-month-old and postnatal day 10 rats. Acute hippocampal slices were subjected to OGD for 2 h followed by 2.5 h reoxygenation. At the end of incubation, slices were homogenized and aliquots were processed for immunoblotting with antibodies against phosphorylated p38 or JNK and total p38 or JNK. (a) Representative images of western blots indicating the p-p38 and p38 levels at 43 kDa in the absence or presence of EUK-207 (50 μmol/L), EUK-207 plus PD98059 (10 μmol/L), or EUK-207 plus SB203580 (1 μmol/L). (b) Quantitative analysis of blots similar to those shown in (a) Results are expressed as percent of control values and the data represent means ± SEM of four experiments. (c) Representative images of western blots indicating the p-JNK and JNK levels at 46 and 54 kDa. (d) Quantitative analysis of blots similar to those shown in C. Results represent means ± SEM of five experiments (PD: PD98059; SB: SB203580).

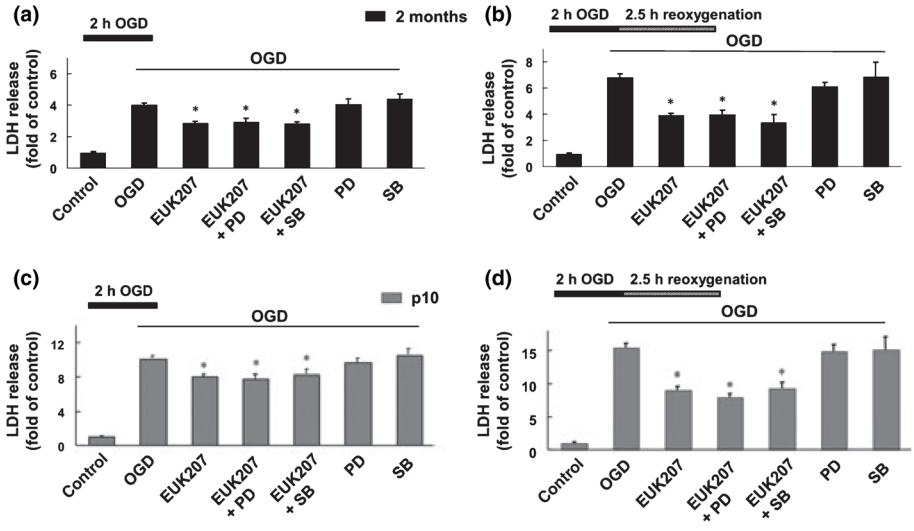

Fig. 8.

Effects of EUK-207, PD98059, and SB203580 on OGD-induced LDH release in acute hippocampal slices from 2-month-old and postnatal day 10 rats. Hippocampal slices from 2-month-old rats were subjected to (a) 2 h OGD or (b) 2 h OGD followed by 2.5 h reoxygenation, in the absence or presence of EUK-207 (50 μmol/L), EUK-207 plus PD98059 (10 μmol/L), or EUK-207 plus SB203580 (1 μmol/L). Results are expressed as fold increase over control values and are means ± SEM of 10 experiments. Hippocampal slices from postnatal day 10 rats were subjected to (c) 2 h OGD or (d) 2 h OGD followed by 2.5 h reoxygenation, in the absence or presence of EUK-207, EUK-207 plus PD98059, or EUK-207 plus SB203580. Results are expressed as fold increase over control values and are means ± SEM of 10 experiments (*$p < 0.05$ as compared to OGD-treated slices, student's *t*-test. PD: PD98059; SB: SB203580).

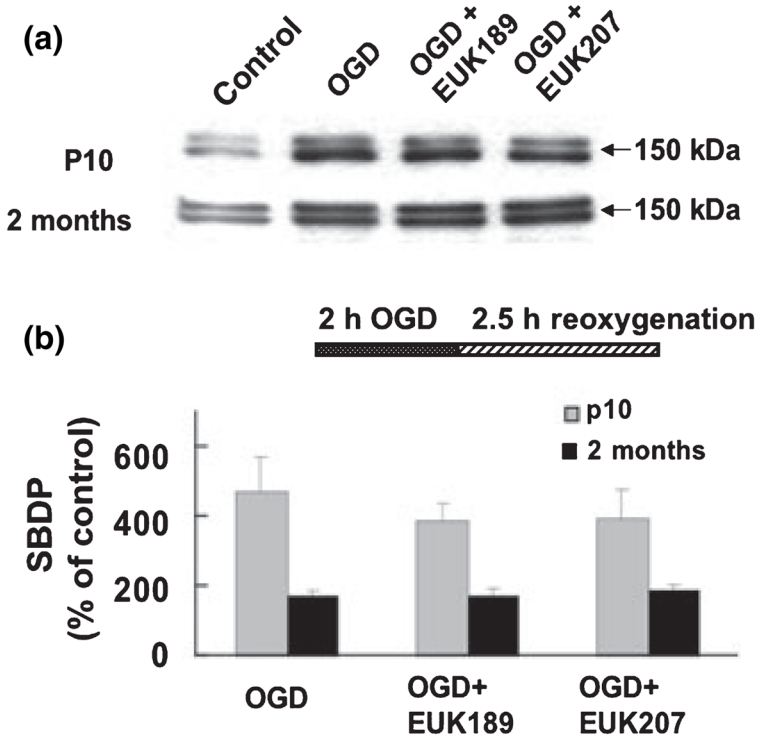

Fig. 9.

Effects of EUK-207 and EUK-189 on OGD-induced calpain activation. Acute hippocampal slices from postnatal day 10 or 2-month-old rats were subjected to OGD for 2 h followed by 2.5 h reoxygenation in the absence or presence of EUK-189 (50 μmol/L) or EUK-207 (50 μmol/L). At the end of treatment, slices were homogenized and aliquots were processed for immunoblotting with spectrin antibodies. (a) Representative images of western blots indicating the levels of calpain-mediated spectrin breakdown products (SBDP) at 150 and 145 kDa in the absence or presence of EUK-189 or EUK-207. (b) Quantitative analysis of blots similar to those shown in A. Blots were scanned and the intensities of SBDP bands were quantified and expressed as percent of control values and the data represent means ± SEM of four experiments.